UNIVERSITÀ DEGLI STUDI DI PADOVA

DIPARTIMENTO DI BIOLOGIA

Corso di Laurea magistrale in Biologia Evoluzionistica

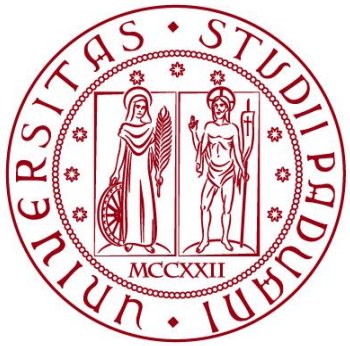

TESI DI LAUREA

Histological Analysis of Enamel Dental Defects in Two Individual Plague Victims from Lazzaretto Vecchio (Venice, Italy)

Relatore: Luca Pagani, Dipartimento di Biologia

Correlatori:
Stefano Benazzi
Gregorio Oxilia
Owen Higgins

Laureanda: Bryn Marie Philiotis

ANNO ACCADEMICO 2021/2022

1. Introduction

Since the start of organized civilization, illness and plague have been both a topic of personal concern and study - including their development, spread, and impact on society at large. Typhoid, diphtheria, cholera, typhus, and other such diseases of the ancient world persisted in Europe throughout time, with one of the most infamous periods of disease being the Middle Ages (O'Neil, 2008). Not only were these known diseases present, but given its cyclical nature, a new wave of the plague would emerge periodically, though with varying intensity. It is frequently suggested that the disease proliferated as a result of close living conditions with rodents, but other proposed causes have included human ectoparasites (Sun et al, 2019; Dean et al, 2018). Regardless, the disease known as "The Plague " is thought to be caused by the bacterium *Yersinia pestis*, though this may not be the case for every plague throughout history (Ell, 1989).

Many pathologies were directly related to diet. While the emergence of more commercial and urban communities allowed better access to grains and fundamental food supplies, it could lead to issues such as dietary deficiencies (O'Neil, 2008). It is known that the medieval diet was heavily based on grains such as wheat and barley, with meat and other foodstuffs making up a smaller part of the diet, though varying depending on the location and local foods (Woolgar, 2006; Lahtinen & Salmi, 2017). Grain-based foods such as porridge and bread became basic food staples that made up the majority of calorie intake for most of the population. In the early Middle Ages, this staple became so fundamental that the proportion of a cereal diet went from about a third to nearly three-quarters from the 8th to 11th century (Hunt & Murray, 1999). During the Renaissance, Europe also saw many dietary changes due to the import of new grains such as corn and potatoes as well as other delicacies such as tea, coffee, and chocolate (Van Hee, 1996). While there were methods for regular teeth cleaning, including the use of pastes and rough linen cloths for brushing (Bifulco, 2016), conditions directly related to care of oral hygiene such as the development of cavities or accumulation of calculus have been recorded in many archaeological populations (Anderson, 2004; Zechini, 2018; Towle, 2017, Djurić-Srejić, 1998). The prevalence of these conditions did, however, also depend on the population and their specific diet (Srejić, 2001). Other conditions such as abscesses, tooth loss, and other periodontal diseases have also been recorded (Djurić-Srejić, 1998; Trombley, 2019; Clark, 1989).

Some of the most common tooth-related pathologies that plagued the Middle Ages and the Renaissance are seen even today. One of these is the cavity, which, in modern-day, is found in nearly half of all children from age two and up (NIDCR, 2018). Both dietary factors and genetic conditions can make one more susceptible to the pathology, but the mechanism is the same – the breakdown of teeth enamel by acid, often through a low pH environment (Zabokova-Bilbilova, 2020). This pathology can be a manifestation of an underlying condition, particularly those that affect the pH of saliva, though one of the most common causes of cavities is a diet high in simple sugars and starches (Touger-Decker et

al, 2008). Simple sugars will immediately cause a decrease in saliva pH, and a diet constantly high in sugar will keep pH chronically low without a chance to recover to a healthy balance (Gupta et al, 2013). A diet high in starches, on the other hand, will cause a less intense pH depression, but the effect of the pH depression is longer. In combination, these two factors can cause long-term susceptibility to cavities. A common hypothesis is that, with the spread of agriculture, there has been a general decline in oral hygiene resulting in tooth decay and cavities, especially due to the cultivation of starches and carbohydrates/sugars (Cornejo, 2010). However, this hypothesis has been contended. Depending on the agricultural crop, the proportion of tooth decay can also vary between populations – for example, even though cavities are commonly found in the remains of Aboriginal populations in Mesoamerica that were cultivating corn, the same cannot be said for populations cultivating rice in central Asia (Tayles, 2000). On the contrary, one hypothesis even suggests that while sugars and starches are one of the primary causes of cavities and tooth decay, it could be the overall lack of a diverse microbacterial ecosystem that increases susceptibility to tooth decay, and so the entire diet should be taken into consideration, not only the amount of sugar (Adler et al, 2013).

Hypoplasia, much like cavities, is a pathology that can have environmental or congenital causes. In all cases, this condition is caused by developmental disturbances which affect the secretion of the enamel matrix, resulting in a deficient enamel quantity or structure (King et al, 2002). Enamel hypoplastic lines, which are linear defects that appear in tooth enamel during crown development, are particularly characteristic of periods of physiological stress such as illness or malnutrition during infancy and childhood (Reid and Dean, 2000; Dabrowski, 2021; Folayan, 2020). These lines can vary in severity, appearing as subtle lines or as clear malformations of the enamel in more severe cases. Malformations may also appear as pitting or otherwise irregular enamel formation. Local trauma and birth injury can also cause this malformation on a single tooth (particularly known as Turner's Hypoplasia or Turner's Tooth). While the cause of the physiological stress may or may not be determined, this condition can be used as a measure for general demographic health and quality of life, even between different groups within a population, such as between males and females (Šlaus, 2000).

Hypoplasia could also be a symptom of a broader genetic pathology or the result of a gene mutation. Known as Amelogenesis Imperfecta, this condition covers a wide variety of malformations in the enamel, including pitting, plane-form effects as well as hypoplasia. This condition is tied to many single mutations in genes controlling the production, thickness, and mineralization of enamel, including the AMELX/AIM1 gene on the X-chromosome and ENAM/AIM2, MMP-20, and Kallikrein 4 on autosomal chromosomes (Wright, 2015). Or, as opposed to being a single mutation, it can be a symptom of more serious hereditary conditions such as Usher Syndrome, Treacher-Collins Syndrome, or Rubinstein-Taybi Syndrome (RTS) (de la Peña et al, 2011; Zanchetta et al, 2018 Cobourne, 2012).

In archaeological studies, teeth with conditions such as these are some of the most useful tools in a set of human remains. Chronological reconstruction can be done on each tooth by analyzing the secretion of the enamel matrix in relation to regular biological rhythms. Circadian growth markers (cross striations) along enamel prisms which appear as a result of the daily enamel secretion pattern, as well as long-period markers (Retzius lines) with circaseptan periodicity (6-12 days in humans) that develop through the regular deposition of enamel layers during crown formation, can be used (Nava et al, 2017; Reid and Dean, 2006). Retzius lines that are darker or accentuated (AL) due to a disruption in the enamel matrix may also represent the occurrence of physiological stress. Enamel prisms can be used to calculate a daily secretion rate (DSR) from one Retzius line to another (MacCord, 2013). This chronological approach begins from the enamel dentine horn and moves along the EDJ until the base of the enamel crown. (Monson et al, 2020). The length of the EDJ between two Retzius lines can be used with the DSR calculated to produce an Enamel Extension Rate (EER), or how fast the crown grows per day (in μm/d) (Guatelli-Steinberg, 2012). Ultimately, if the neonatal line (marking the moment of birth) is absent, in conjunction with average crown initiation and completion times, information including the age of the tooth, the age of the individual, and the timing of physiological stresses may be observed.

2. Archaeological Context

The Italian plague of 1630-1631 in Venice particularly is one of the most carefully documented plague epidemics in Europe. Most parishes recorded plague deaths, among other deaths, of each person as well as their name and surname, age, occupation, days of illness, and place of residence. Even more impressive is that all individuals were recorded - including non-Venetians or immigrants, both sexes, and adults and children (Ell). As a result, epidemiologists and historians can track how the plague spread throughout the city with great confidence, how many deaths were taking place each day, and who was being affected the most.

Many of the precautions that were seen in the rest of the country were being taken, including quarantining and movement restrictions, especially when it came to docking boats. However, as the plague likely entered the mainland from the mountains, there was little that could be done to prevent the spread of the plague into the city. Once present, plague regulations simply failed as the city was so well connected and densely populated. As a result, with the parallel increase of mortality due to the synchronous smallpox epidemic, rise in public violence, and indirect effects of the plague, the plague caused a societal and demographic upheaval, and the city saw a nearly 33% decline in its local population in a single year (Ell, 1989).

Despite the difficulty in stopping the spread of the plague, Venice did have a unique advantage – as a city made up of many islands, it was easy to implement isolated units for the treatment and burial of plague victims. In 1423, the island Santa Maria di Nazareth, originally housing a church as a shelter for pilgrims, was delegated to become a specialized hospital for the treatment and isolation of people with the plague. Sequentially, in 1468, the island Vigna Murada was used as a quarantining center for merchants, sailors, and goods entering the city. Following the institution of the second lazarette, the two islands were hence known as Lazzaretto Vecchio and Lazzaretto Nuovo, respectively.

After the plague, both lazarettes were turned into military deposits due to their strategic position in the Venetian lagoon, with most medieval buildings being torn down. Since their decommissions in the mid-20th century, both islands reverted to become remarkable archaeological sites and popular tourist locations.

While Lazzaretto Nuovo is well known for its historical buildings, artworks, and writings, Lazzaretto Vecchio is particularly useful in studying the plague of 1630 and its victims. Since then, the islands have remained in a state of neglect until restoration works began in the early 21st century, intending to recover their structures and integrate the islands into the National Archeological Museum of the Venetian Lagoon. In fact, in 2005, over one hundred burial pits were excavated, revealing hundreds of plague victims. Due to the high fatality as well as the prejudices against plague victims, individual victims were often not granted the leisure of a proper singular burial, and so for many, mass burials are their final resting place.

Lazzaretto Vecchio is an island in the central area of the Venetian Lagoon, situated off the western coast of Lido in the northern Italian province of Veneto. The island covers an area of approximately 2.53 hectares (6.3 acres). Since 2004, more than 1500 skeletons of plague victims buried between the 15th and 17th centuries have been excavated (Valsecchi, 2007). These individuals were excavated particularly in February and March of 2005. They belong to the period of the 1630-1631 plague of Venice, which is affirmed based on dating related to ceramic finds within the pits and stratigraphic relationships that these pits have with other pits in the area.

Here we study two individuals recovered from Lazaretto Vecchio in Venice, Italy, dated to the period of the 1630 plague. Histological analysis was focused on the upper right canine (URC) and the second upper right incisor (URI2) of individuals 1 and 2, respectively. Not only can these teeth give insight into the age of the individual, but aspects represented through the crown's enamel can also give a precise insight into daily life - including diet, illness, and even culture, at this particular point in time.

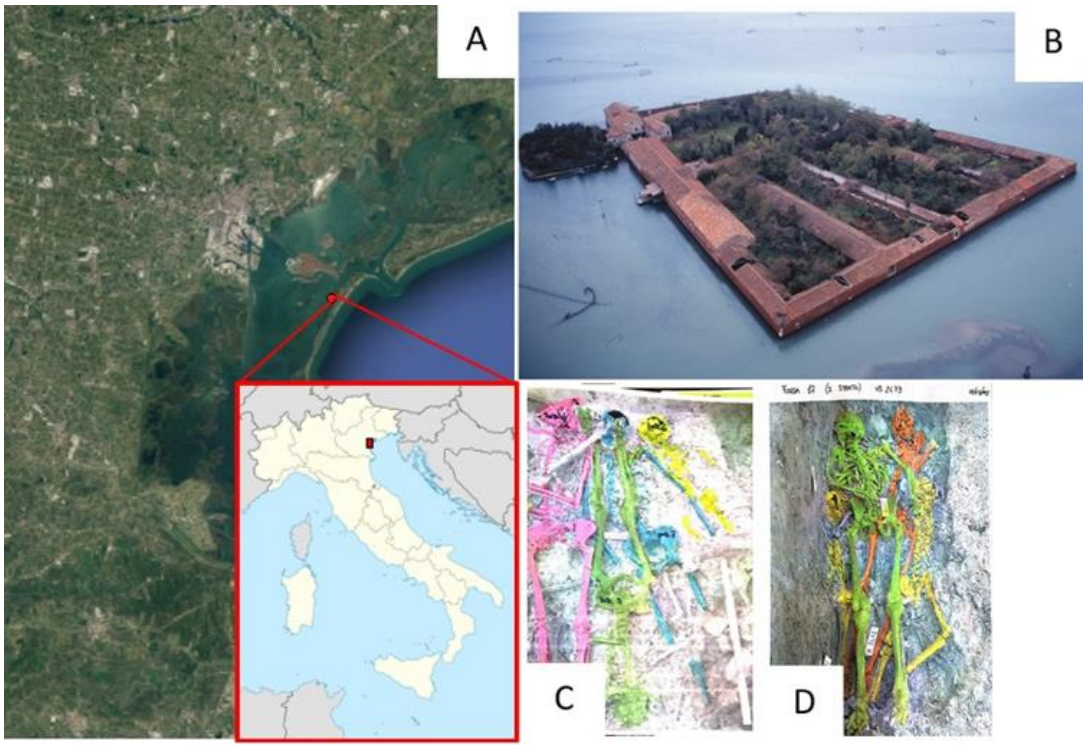

Fig. 1: (A) Map of the region of Venice and its location in Italy. (B) Aerial view of Lazzaretto Vecchio. (C) Orientation of individuals found in Pit 97 - Individual 6 highlighted in yellow, at the bottom right of the image. (D) Orientation of individuals found in Pit 17 - Individual 1 highlighted in green, in the center of the image.

3. Objectives

Many pathologies have been shown to cause lasting effects on the masticatory system, particularly if contracted during tooth development. These periods of physiological stress can be visualized through enamel hypoplasia and variance in enamel growth rates. With this in consideration, when studying archaeological sites, we may be able to use teeth from a variety of remains to examine and estimate the general health of past populations. In the context of Lazaretto Vecchio, a site for quarantine, treatment, and mass burial during the Venetian Plague of 1630, skeletal biomarkers may be used as indicators of physiological stress, including those due to the plague. Biomarkers such as the presence of cribra orbitalia, hyperostosis, and hypoplasia are frequently used as identifiers of physiological stress (Bramanati, 2018). Due to the poor condition or the young age of many remains, however, the use of cribra orbitalia in severely fragmented remains or hyperostosis for teeth with incomplete roots may not be the best criteria, but the use of hypoplasia as the sole method of stress determination may be sufficient.

Two individuals, a juvenile female and an infant, were chosen based on their particularly extreme enamel hypoplasia. They may represent a unique opportunity to study the impact of physiological stresses on teeth enamel in a Medieval/early modern context in Venice, Italy.

4. Materials and Methods

4.1 Materials

Individual 1, US 2473 Pit 17, Level 1

Individual 1 (hence referred to as I1) was excavated from the first level (of two levels) of Pit 17 of the southern section of Trench 2B (Figure 1, C) It was found with five other individuals in total, three of which were on the same level. It was found almost entirely complete, only missing the most distal phalanges of the fingers and toes. The individual was found leaning towards the second layer, covering Individual 2, oriented east-west in the middle of the pit with the body and legs extended straight and upper limbs extended along the body. While this individual was nearly complete when discovered, it appears that at some point along the process from excavation to lab analysis the majority of the left half (including the left upper and lower limbs, hands, feet as well as pelvis) was lost. For the histological analysis, the upper right canine (URC) was selected.

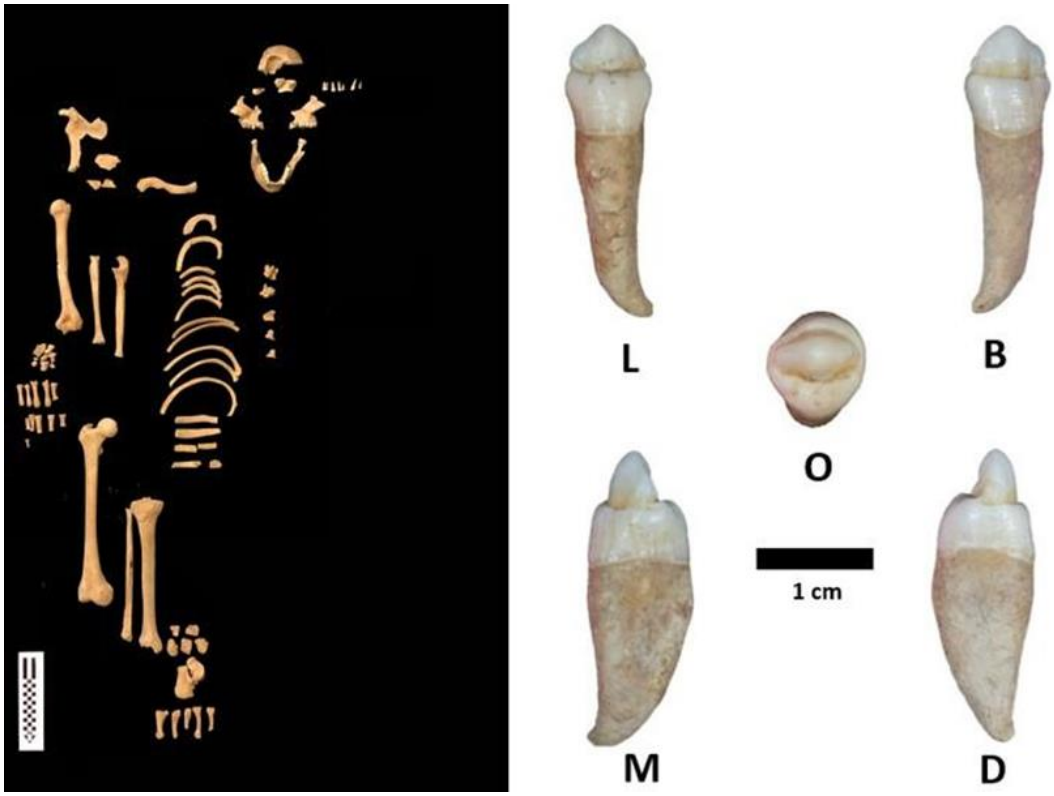

Fig. 2: Completed skeletal remains of Individual 1 (left), views of the upper right canine (right).

Individual 6, US 4084 Pit 49, Level 1

Individual 6 (hence referred to as I6) was excavated from the first level (of three levels) of Pit 97 of the southern section of Trench 2C (Figure 1, D). It was found with 22 other individuals, 5 of whom were on the same level. It was found mostly fragmentary and in relatively poor condition, with the hands, feet, and lower arms and legs completely absent. The individual was found on the bottom of the pit on the eastern border, oriented north-south from head to foot. For histological analysis, the upper right second incisor (URI2) was selected.

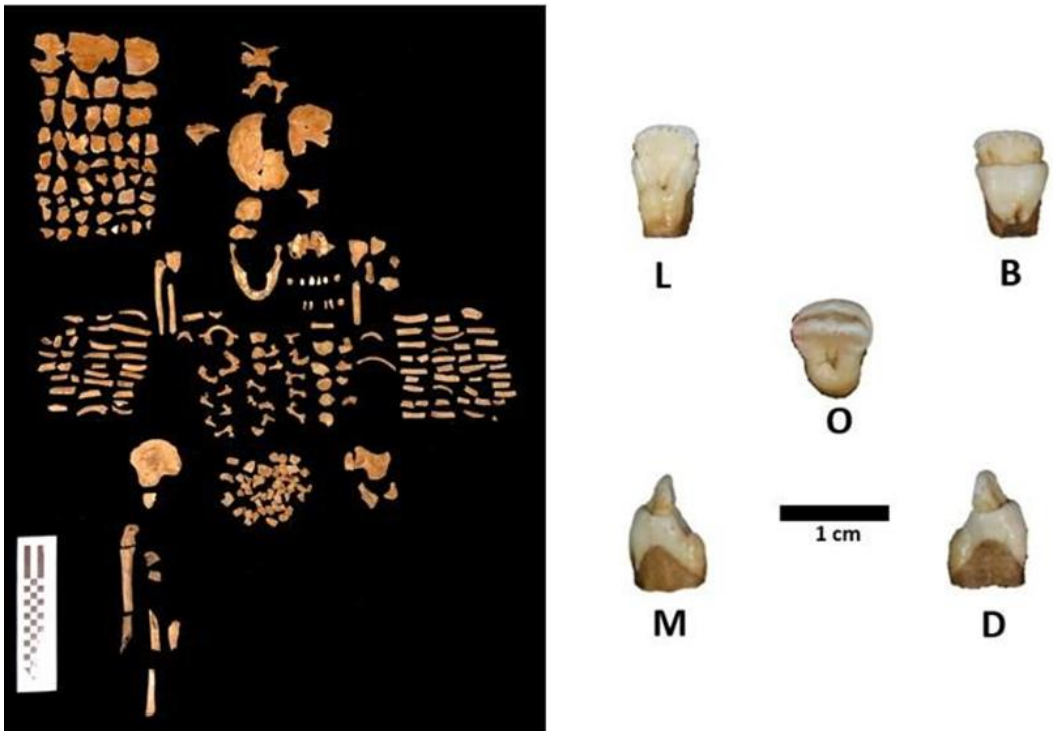

Fig. 3: Completed skeletal remains of Individual 6 (left), views of the second upper right incisor (right).

4.2 Osteoarchaeological Analysis

The remains were cleaned and restored at the Osteoarcheology and Paleoanthropology Laboratory (BONES Lab) using a soft nylon brush and water. Anatomical identification of the remains was then conducted to reconstruct the biological profiles. Any fragmented remains that could be identified and restored were done so by gluing them together with Artiglio® Casa Trasparente transparent adhesive. Estimating the age of death of the individuals was based on the following methods: level of epiphyseal closure and/or fusion of ossification centers (Schaefer et al, 2009; Webb and Suchey, (1985); Garn et. al, (1967); Cardoso, 2008; Coqueugnoit and Weaver, 2007), dental development, eruption, and wear (Alqahtani, 2010; Hillson, 1996), and measurement of total and/or diaphyseal length (Maresh, 1970; Scheuer and Black, 2000;). Pathological profiles were completed by determining the presence or absence of pathologies through macroscopic examination with the aid of a magnifying glass using (Ortner, 2003) and (White and Folkens, 2005). Upon profile completion, the remains were then photographed in their entirety. Further detailed analysis of the teeth was completed through individual identification of all teeth and the creation of a dental profile. The URI2 of I6 was already separated from the maxilla, but the URC of I1 was intentionally removed from the maxilla for further detailed analysis. Photos were then taken of these two teeth, as well as other photos detailing other teeth and the maxillae and/or mandibles.

4.3 Acquisition and post-processing

The URI2 of I6 and the URC of I1 were photographed from all views using a Fujifilm X-T3 digital camera. High and low light photos were also taken of all views and specific details using a Leica s9i Microscope with Greenough Stereo Zoom between 0.61 and 5.5x, with the program Leica Application Suit X, version 3.0.1423224. High-resolution multi-focus mosaic photos of the surface of the teeth from all views were taken in polarized reflected light with a Carl Zeiss Axioscope 7 microscope with a Carl Zeiss Axiocam 208 Color camera with a 10x objective lens, and Zen Core software (Carl Zeiss AG, Oberkochen, Germany) to automatically construct the mosaics. Finally, the URC and URI2 were analyzed by X-ray microCT at the Department of Physics and Earth Science of the University of Ferrara. The scanning procedure was performed using a microFocus x-ray tube (Hamamatsu L9421, minimum focal spot size 5 μm) at 70 kVp, 0.1 mAs, 0.5 mm Al filtration, 360 projections over 360°, for a total scan time of 20 minutes. The tomographic images were reconstructed using an FDK algorithm after the application of beam hardening correction. The reconstructed volume has a linear voxel size of 30 μm. The microCT images of the original samples were virtually segmented using Avizo 9.2 software (Thermo Fisher Scientific, Waltham, Massachusetts, US). The segmented enamel caps and virtually filled dentin were converted to meshes using Geomagic Design X (3D Systems Software, Rock Hill, South Carolina, US), a 3D metrology software (Fig. 4). The 3D models were then prepared and the enamel and dentine/root were compiled into separate layers.

4.4 Histology

Histological analysis of the teeth was then performed on the URC and URI2 of I1 and I6, respectively. This analysis was conducted by analyzing the histomorphometry of the teeth to determine factors such as age at death and signs of stress and/or pathology. The teeth were prepared by embedding them first in Aremco Crystalbond 509-3 (to allow for extraction after tooth cutting) and then in Buehler Epoxy Resin by mixing EpoThin 2 Epoxy Resin and Epoxy Hardener in a 4:1 proportion. Each tooth was initially cut along the buccolingual axial plane passing through the dentine horn (identifying its position from the microCT images and the 3D virtual reconstruction of the teeth) by using a Buehler IsoMet Low Speed Saw with a diamond wafering blade of 0.3 mm of thickness. The cut surface of the most appropriate resulting half was then ground with P2500 abrasive paper and polished with 1 µm MetaDi Polycrystalline diamond suspension (Buehler). The polished blocks were then rinsed with demineralized water and attached to a glass slide using EpoThin 2 (Buehler) Epoxy Resin, at which point a thin section was cut using a Buehler IsoMet Low Speed Saw with a diamond wafering blade of 0.3 mm of thickness. The thin sections were then ground using a target holder on P1200 grit abrasive paper until 300 micrometers of thickness, and P2500 grit abrasive paper until 180 micrometers. The sections were then polished with 1 µm MetaDi Polycrystalline diamond suspension (Buehler) and photographed using the same Carl Zeiss Axiocam 7 and camera mentioned in "Acquisition and post-processing" (4.3). A mosaic picture of each section was compiled using the mosaic feature of Zen Core 3 software (Carl Zeiss AG, Oberkochen, Germany) and exported in .tif format. The .tif files were then opened in Adobe Photoshop and a ca. 100 µm line was traced following the direction of the enamel prism that started from the EDJ (Enamel Dentine Junction) at the dentine horn. Tracing a second line from the end of the first, the relative Retzius line was followed until it met the EDJ and so forth, repeating the process until the cervical area of the crown was reached. The estimation of local DSRs was attempted, but in many areas of both teeth the daily cross striations were not discernable. The visualization ability of cross striations did not change with focus adjustment through the microscope.

The building of the chronological framework was necessary to estimate the biological rates of enamel deposition and to construct a chronology for the life history of the individuals under analysis. The length of the EDJ was taken in Fiji software after having set the appropriate scale involved. As daily cross striations could not be identified regularly, local DSRs could therefore not be measured, and so a standard DSR was used for both teeth: 3.12 µm per day for the canine, based on the average between medieval and modern canine samples from the work of Aris (2022), and 2.85 µm per day was used for the incisor, based on the works of Guatelli-Steinberg et al (2012).

For the URC of I1, the hypoplastic event was present on both the lingual and buccal sides. Chronological reconstruction before and after the hypoplastic event period was calculated using the length of the EDJ between two Retzius lines over

the standard DSR to find the number of days between the two. The EERs were calculated by dividing the length of the EDJ between two Retzius lines and the number of days elapsed between the formation of the two.

The period of the hypoplastic event was estimated using the proportion between the total length of the EDJ and the length of the EDJ between the start of the hypoplastic gap and when enamel deposition resumed in relation to the total days of crown formation and the time passed between the two points. This can be represented in the following formula:

$$Total\ EDJ\ Length : EDJ\ Length\ During\ Hypoplasia = Total\ Days\ of\ Crown\ Formation : Time\ Passed\ Since\ Hypoplastic\ Event\ Beginning\ to\ End$$

The crown was also divided into 10 deciles using the length of the EDJ to find the position of the hypoplasia and its length relative to the EDJ length. The same methods were used to calculate the chronological gap, and represented by the following formula:

$$Total\ EDJ\ Length : EDJ\ Length\ During\ Hypoplasia = Total\ Days\ of\ Crown\ Formation : Time\ Passed\ Since\ Hypoplastic\ Event\ and\ Nearest\ Retzius$$

The chronological gap and hypoplastic gap were calculated for both the lingual and buccal sides, but only the buccal side was considered when estimating the final chronology.

A second method to calculate the chronological gap was done by taking the length of the EDJ between the initial hypoplastic event (AL 10) and the most recent Retzius line after enamel deposition resumed. This length was divided by the average EER between the two points to find the total amount of days that passed.

For the URI2 of I6, the cuspal and initial lateral areas of the lingual side were used for chronological reconstruction, as the hypoplastic event did not cause an interruption of enamel secretion in this area, unlike on the buccal side. This allowed us to overcome the problems caused by the gap in enamel deposition for the reconstruction of the chronology by uniting the two chronologies through the identification of specific synchronous moments, being the ALs that formed after the hypoplastic event. The buccal side was then used for chronological reconstruction after the hypoplastic event, as the Retzius lines were predominantly visible only on that side. Chronological reconstruction was done in the same manner as the URC, in which the length of the EDJ between two Retzius lines over the standard DSR was used to find the number of days between the two and EERs were calculated by dividing the length of the EDJ between two Retzius lines and the number of days elapsed between the formation of the two.

5. Results

5.1 Osteological Analysis

Individual 1

The individual was estimated as female, primarily based on the mandible, which has a rounded and gracile shape (White and Folkens, 2005) (Fig. 4), supporting the observations as recorded during the original excavation. Any other sexual dimorphic characteristics that would normally be used, such as the ilium or skull (White and Folkens, 2005), were either too fragmented or lost, likely during their transition from the site to the lab.

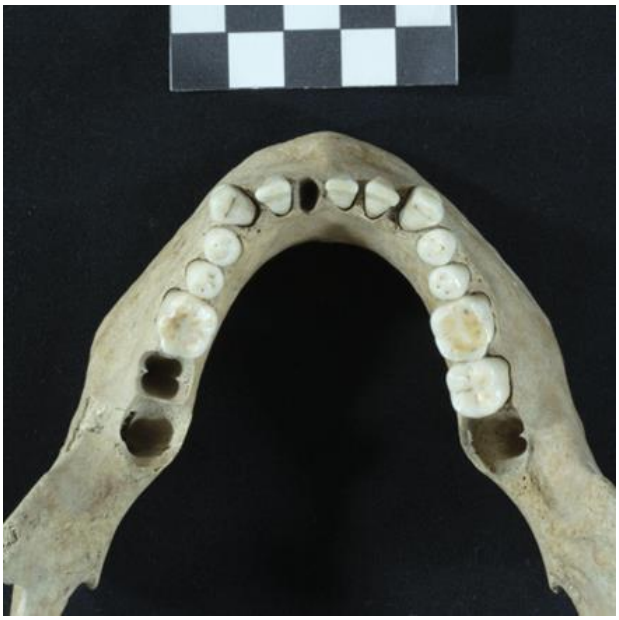

Fig. 4: Mandible of I1 from occlusal view

The individual was estimated to be around 18 years of age based on the stage of teeth eruption and wear (using data from AlQahtani, 2010; Moorrees, 1963; Brothwell, 1981), as well as bone ossification (using data from Schaefer et al, 2009; Webb and Suchey, 1985; Garn et. al, 1967; Cardoso, 2008; Coqueugnoit and Weaver, 2007). The lower right third molar (Figure 6A) had just erupted, with an incomplete root (stage R3/4), suggesting an age between 15.5 and 20.5 years. (AlQahtani, 2010; Moorrees, 1963). While there is no wear on the upper canines, given their angular position and the fact that both the bottom left and right canines have already fully erupted, the upper canines were likely obstructed and prevented from erupting naturally (Figure 5 B, C). All other teeth that are dislodged from their socket are permanent teeth that have erupted and have completed roots. Both the upper and lower first molars also show wear between stages 2+ and 3- (Figure 4), suggesting a similar age between 17 and 25 (Brothwell, 1981).

Fig. 5: A: Lower right third molar of I1 showing incomplete root. B: Original position of the URC in the maxilla of I1. C: Lower teeth as they were originally presented in the mandible of I1

The ossification of the clavicle and upper and lower limbs support this age as well (Fig. 6), with an estimation between 16 and 20 years (Webb and Suchey, 1985; Garn et al., 1967; Cardoso, 2008; Coqueugniot and Weaver, 2007). The length of the skeletal elements (reported in Table 1), primarily that of the upper and lower limbs, suggests an age between 10 and 12 years of age when considering both averages and lower percentiles (Black and Scheuer, 1996; Maresh, 1970). The age estimation based on the length of the bones and ossification degree is compiled in Table 1, and the ossification of the tibial and femoral heads can be seen in Figure 6.

Bone	Total Length (mm)	Age Estimation Based on Length (Years)	Age Estimation Based on Ossification (Years)
Clavicle	30	15-16	16-17
Humerus	300	13	20
Radius	203	11-12	18-21
Ulna	229	12	16-19
Femur	430	12-13	16-18
Tibia	350	11-12	19-20
Fibula	x	x	19-20

Table 1: Total length of bones and the age estimation of Individual 1 based on the length and the degree of ossification of each element. The fibula was incomplete, but ossification could be determined due to complete ossification between the lower extremity and a portion of the main body.

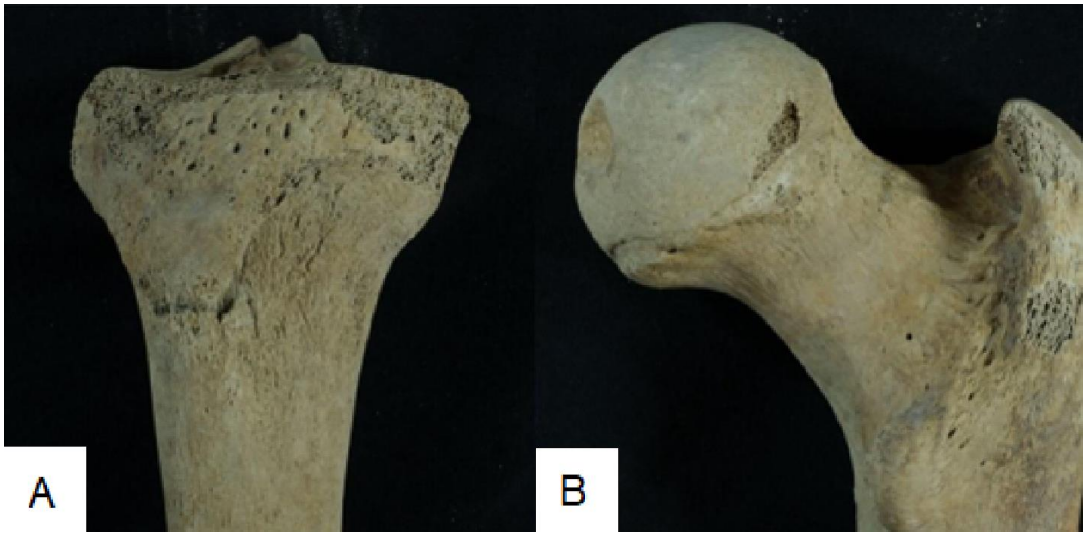

Fig. 6: Ossification of the tibial head (A), ossification of the femoral head (B) of I1

Pathologies were also detected. In Figure 7, it is possible to appreciate the porosity on the right tibia (Fig. 7A) and fibula (Fig.7B), with specifically older spots on the tibia and fibula and new spots on the tibia. The right fibula also has light denting (Fig. 7C), which suggests healed trauma (Ortner, 2003).

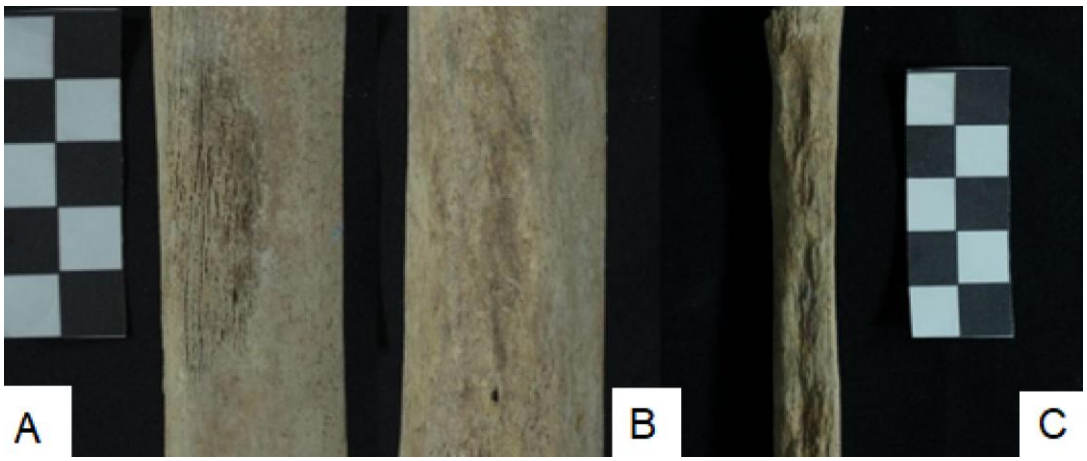

Fig. 7: Porosity on the right tibia (A), porosity on right fibula (B), and denting on right fibula (C) of I1

This individual also appears to be affected by dental abnormalities on all teeth. The teeth are generally affected by hypoplasia and ridging around the entirety of the crown, with the lower canines being particularly affected (Figure 8).

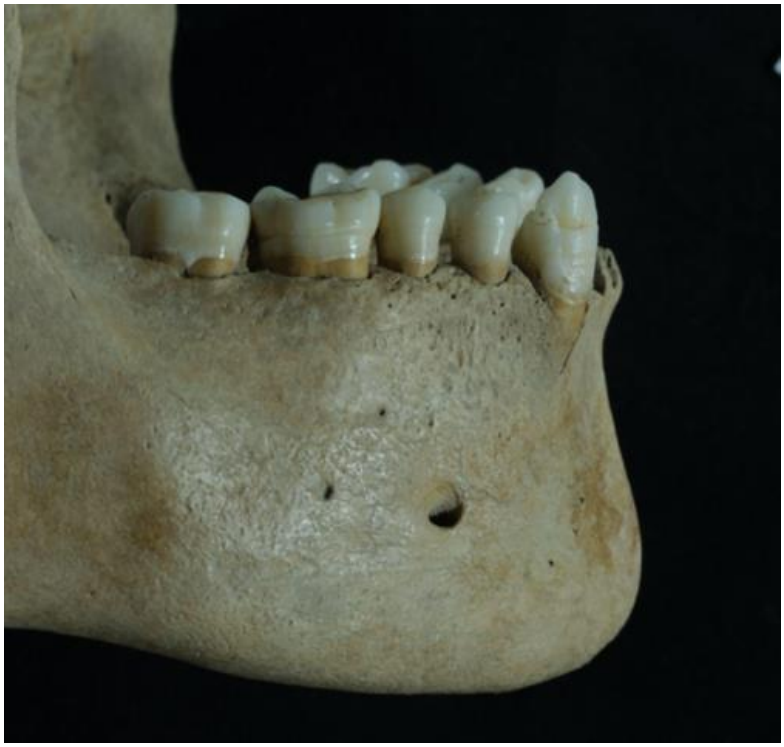

Fig. 8: Right side of the mandible of I1 with teeth, particularly illustrating the hypoplasia on the enamel.

The upper right canine (URC) of this individual, which was used for histological analysis, features a strong linear hypoplastic event in the middle of the crown. The enamel before the linear hypoplasia is a normal thickness, while after the hypoplasia it is considerably thinner (Figure 9B). On the occlusal/buccal end, an irregular patterning of enamel deposits results in a thickened drip-like form (Figure 9A).

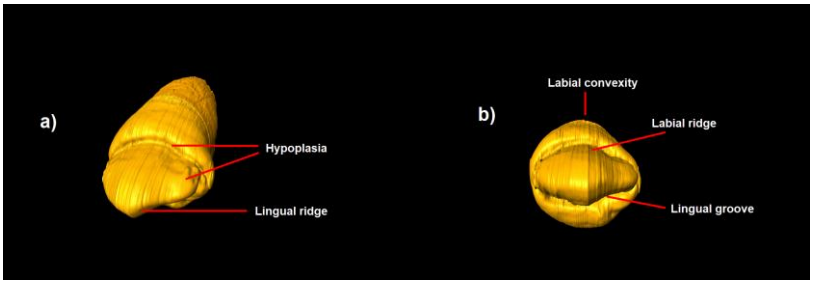

Fig. 9: Completed 3D mesh of URC of I1 from the occlusal/buccal view illustrating hypoplasia (a) and occlusal view of the URC of I1 showcasing the differentiation in thickness before and after the hypoplastic event (b)

Individual 6

The individual was estimated to be around 7.5 – 8.5 years old, solely based on the stage of tooth eruption and completion (AlQahtani, 2010; Moorrees, 1963). Several examples can be seen in Figure 10. The deciduous canines and first and second deciduous molars are still present, while the first permanent molars have fully erupted. The second permanent molars have begun forming and the enamel crowns are completed and have a defined pulp roof (CRC) but have not erupted. The permanent canines have also not erupted, but the upper right canine which has become loose from the mandible has an incomplete root (RI - RI 1/4). The lower left second permanent incisor also has an incomplete root but has erupted (RI 1/4). The other lower incisors have also erupted, but their degree of root completion cannot be estimated as they remain embedded in the mandible. Given the poor condition of the remains and the age in which any ossification that would occur after puberty has not yet occurred and ossification that occurs shortly after birth has long since occurred, only the teeth could be used as an accurate means of aging.

Fig. 10: Deciduous canine and molars (first and second) and first permanent molar of I6 (A). Developed adult second molars of I6 without root (B). Upper first and second incisors of I6 with incomplete roots (C).

Similar complications don't allow the estimation of the sex of the individual on a morphological basis. The individual has not yet reached puberty, and so the common characteristics used to determine sex are not present. No skeletal pathologies were detected, but given the fragmentary and incomplete remains, it is possible that they simply aren't detectable. There is, however, a detectable dental pathology. The individual has several mamelon incisors which are particularly large and flat, and canines that show ridging. All teeth also have noticeable vertical lines and some show extremely defined hypoplastic lines, especially in the upper lateral incisors and lower left first molar (Figure 11). The molars also have particularly high, pointed cusps. Three cavities are also present in the lower right, upper left, and upper right first deciduous molars.

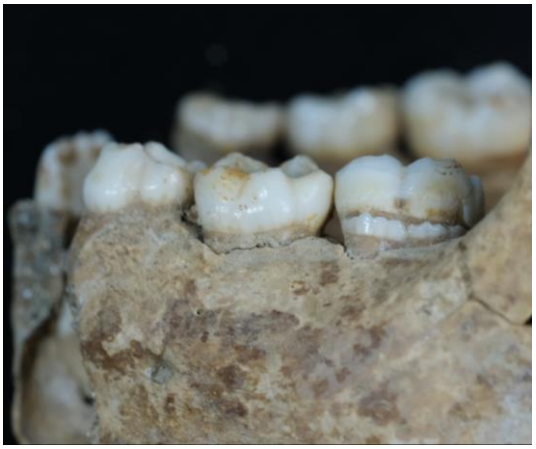

Fig. 11: Left side of the mandible, illustrating the defined division (hypoplasia) within the crown and vertical lines ascending from the base of the root.

The second upper right incisor (URI2) of this individual, which was used for histological analysis, features a strong linear hypoplastic event in the middle of the crown. The enamel before the linear hypoplasia is a normal thickness, while after the hypoplasia it is considerably thinner (Figure 12A). On the occlusal/buccal end, an irregular patterning of enamel deposits results in a thickened drip-like form (Figure 12A). The tooth also features a tubercle with shoveling on the lingual aspect, with many instances of pitting also on the lingual aspect, especially on the tubercle, near the hypoplasia and within the shoveled enamel, and three instances towards the occlusal end (Figure 12B).

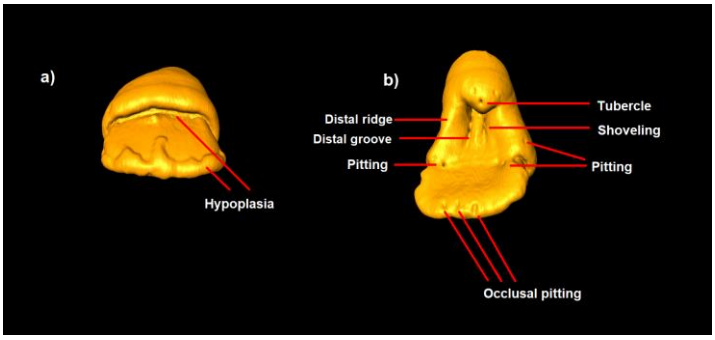

Fig. 12: Completed 3D mesh of URI2 of I6 from the occlusal/buccal view illustrating hypoplasia and showcasing the differentiation in thickness before and after the hypoplastic event (a) and lingual view of the URI2 of I6 showcasing the tubercle, shoveling, pitting events, and slightly "scalloped" mesial and distal aspects (b)

5.2 Histology

The final 3D models created through image segmentation, which feature the buccal, lingual, mesial, distal, and occlusal views plus the form of the EDJ of the root/dentin of the URC of I1 and URI2 of I6 can be seen in Figure 13, below.

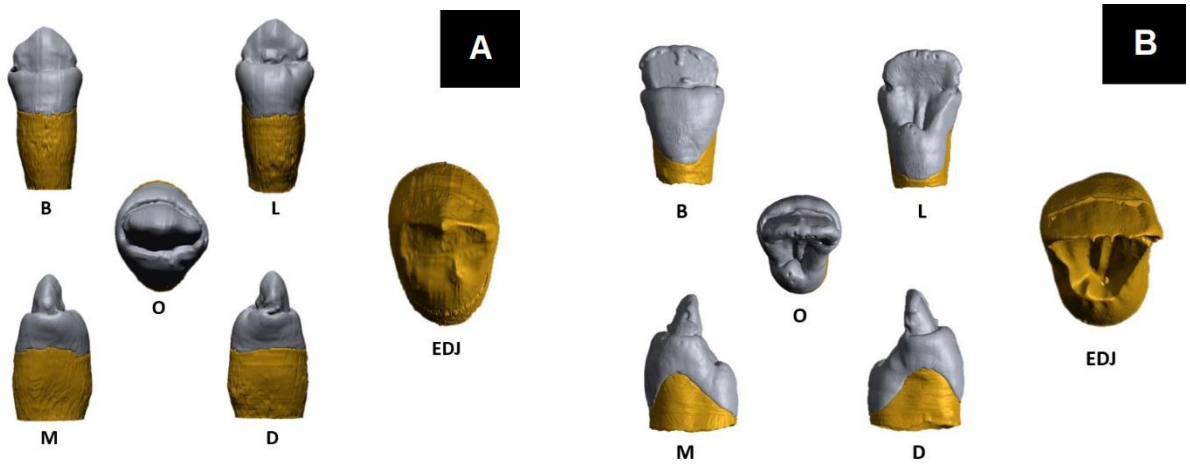

Fig. 13: Completed 3D models of the URC of I1 (A) and URI2 of I6 (B) from different views, plus the form of the EDJ. B = Buccal, L = Lingual, M = Mesial, D = Distal, O = Occlusal, EDJ = Enamel-Dentine Junction

The histological thin section of each tooth, which passes through the buccolingual plane, is shown in Figs. 15 and 16. The direction and orientation of the Retzius lines and accentuated lines (ALs) are well-defined and relatively clear throughout the enamel crown of the incisor, although more so in certain areas than others. For the URI2 of I6, many prisms were clear with defined cross striations, but in some areas few to none were able to be measured. For the URC of I1, only the direction of the prisms is clearly visible, while the cross striations representing the daily deposition of enamel were difficult to discern.

Tables 3 and 4 report the ALs and their estimated time of emergence during the crown formation period, the time before or since the hypoplastic gap (for URC) or initial hypoplastic event (URI), and the estimated time since birth. The estimated time since birth was calculated based on the crown formation time using the work of Reid and Dean (2006). While other Retzius lines were used for chronological estimation, they are not included in the tables as they do not illustrate any physiological stress events.

Both teeth also have “protuberances” occurring after the hypoplastic event and project from the dentine towards the enamel, creating a curved EDJ at the time of stress. These protuberances can be seen in Figure 14, below.

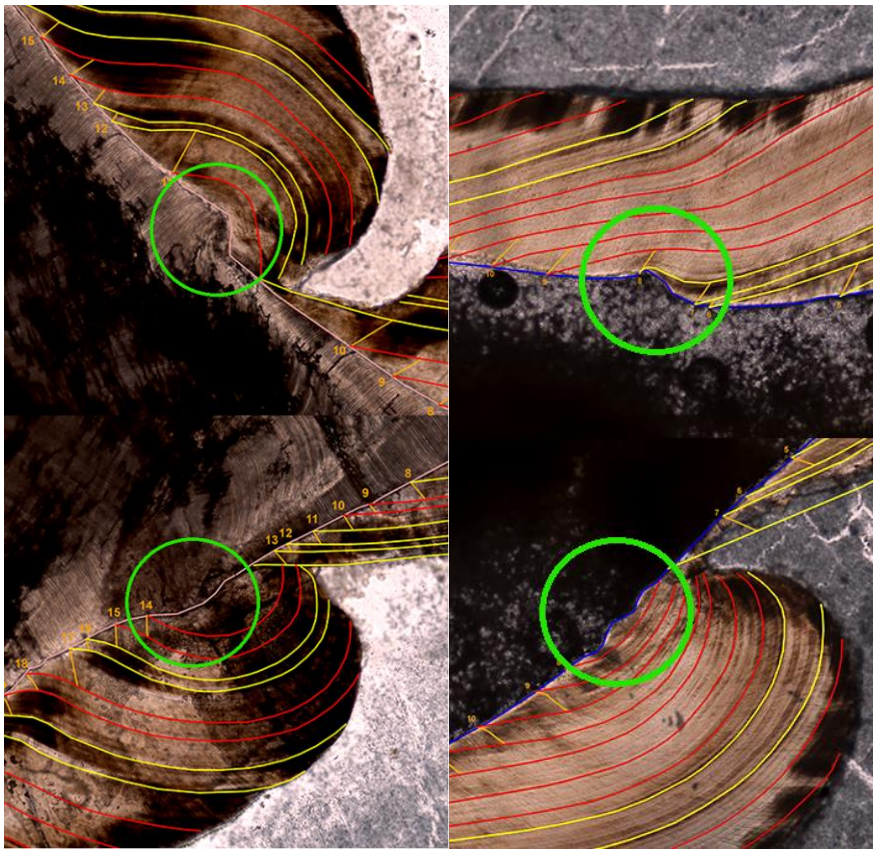

Fig. 14: Circled in green: dentine protuberances that project towards the enamel after the main enamel hypoplastic event. Left: URC of I1 (top: lingual, bottom: buccal). Right: URI2 of I6 (top: lingual, bottom: buccal).

Individual 1

In the crown of the URC, sixteen clearly discernible Accentuated Lines are observable in total. 9 pre-hypoplastic accentuated lines were identified (ALs labeled 1-9), one of which were only on the buccal side (ALs labeled 6). AL 10 corresponds to the hypoplastic event on the buccal side. Post-hypoplastic accentuated lines include five that correspond on both the lingual and buccal (ALs labeled 11-15) and one that is only visible on the lingual side (AL labeled 16). The resulting histological section with traced Retzius and accentuated lines can be viewed in Figure 15. Figure 18 graphs the distribution of ALs from the beginning to the end of crown formation. The distribution of ALs is relatively frequent and regular since birth and occurs both before and after the hypoplastic event, with fewer ALs towards the end of crown development.

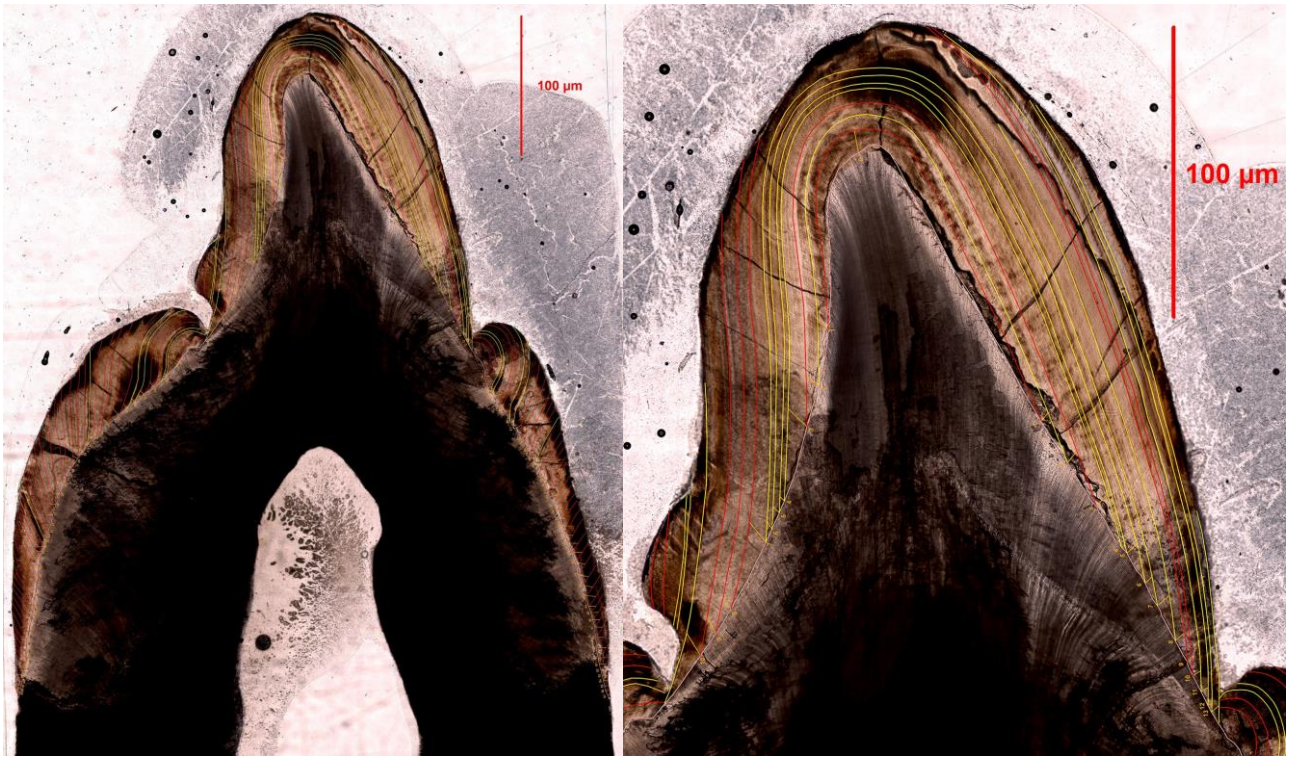

Fig. 15: Histological section of the upper right second canine (URC) of Individual 1. Left: view of the complete enamel crown. Right: view of the cuspal portion in which the hypoplastic event is visible.

The average crown initiation time reported for the URC (274 days) by Reid and Dean (2006), was added to the timing of the hypoplastic event estimated by histologic analysis (356 days; Table 3); the hypoplastic event occurred at age 630 days / 1.7 years. The total length of the EDJ equaled 10.3 mm over 1708 days, not including the time that passed during the chronological gap due to hypoplasia.

The chronological gap induced by the hypoplasia was estimated using the following equation:

$$Total\ EDJ\ Length : EDJ\ Length\ During\ Hypoplasia = Total\ Days\ of\ Crown\ Formation : Time\ Passed\ Since\ Hypoplastic\ Event\ and\ Nearest\ Retzius$$

Using the data, this equates to:

$$10321.6 : 433.9 = 1709.5 + x : x$$

where x equals the time passed since the hypoplastic event and the first identified Retzius line after enamel deposit resumption. In sum, this corresponded to 75 days. The same method was used to calculate the length of the period from the initiation of the hypoplastic event to the enamel deposit resumption:

$$Total\ EDJ\ Length : EDJ\ Length\ During\ Hypoplasia = Total\ Days\ of\ Crown\ Formation : Time\ Passed\ Since\ Hypoplastic\ Event\ and\ secretory\ resumption$$

Using the data, this equates to:

$$10321.6 : 224.0 = 1709.5 + x : x$$

In sum, this corresponded to 37 days. The tooth's decile was calculated using the total length of the crown's EDJ (10.3 mm). Its length when the hypoplasia occurred was 4.8 mm, and the first identified Retzius line after enamel production resumed was 5.3 mm. 47% of the crown was completed at the start of the hypoplastic event. By the resumption of enamel deposits, 49% of the crown was completed, and up to 51% was completed by the first identified Retzius line after enamel production resumed.

Using the same methodology for the lingual side, the hypoplastic event also occurred when the EDJ length was 5.3 mm, or when 46% of the EDJ length was completed. Enamel production resumed at 49% of EDJ length, and up to 51% was completed by the first identified Retzius line after enamel production resumed. Using the same formulas as above, the chronological gap was 80 days and the period from the initial hypoplastic event to when enamel deposit resumed was 41 days.

By using the length of the EDJ between the hypoplastic event and the first identified Retzius line after the enamel deposit resumption and the EER, it is estimated that 93 days passed between the two points for the buccal side, and 86 days passed between the two points on the lingual side.

According to the chronology calculated on the buccal side, the crown had completed at 59 months / 4.9 years after crown initiation, or 5.6 years after birth when adding the crown initiation time of Read and Dean 2006 (274 days). Such estimation is consistent on the lingual side, also reporting crown completion at 5.6 years.

Individual 6

In the crown of the URI2, fourteen clearly discernible Accentuated Lines are observable in total - six lines on the cusp / on the lateral and buccal sides before the hypoplastic event (ALs labeled 1-6), the beginning of the hypoplastic event (AL labeled 7) three which correspond to both the lingual and buccal sides and are the first accentuated lines after the hypoplastic event (ALs labeled 8-10), and four that are visible only on the buccal side (ALs labeled 11-14). AL 7 on the lingual aspect corresponds to the hypoplastic event on the buccal side. The resulting histological section with traced Retzius and accentuated lines can be viewed in Figure 16. Figure 19 graphs the distribution of ALs from the beginning to the end of crown formation. There is a concentration of ALs around four months before the hypoplastic event, with another peak of ALs occurring between 14 and 15 months after such.

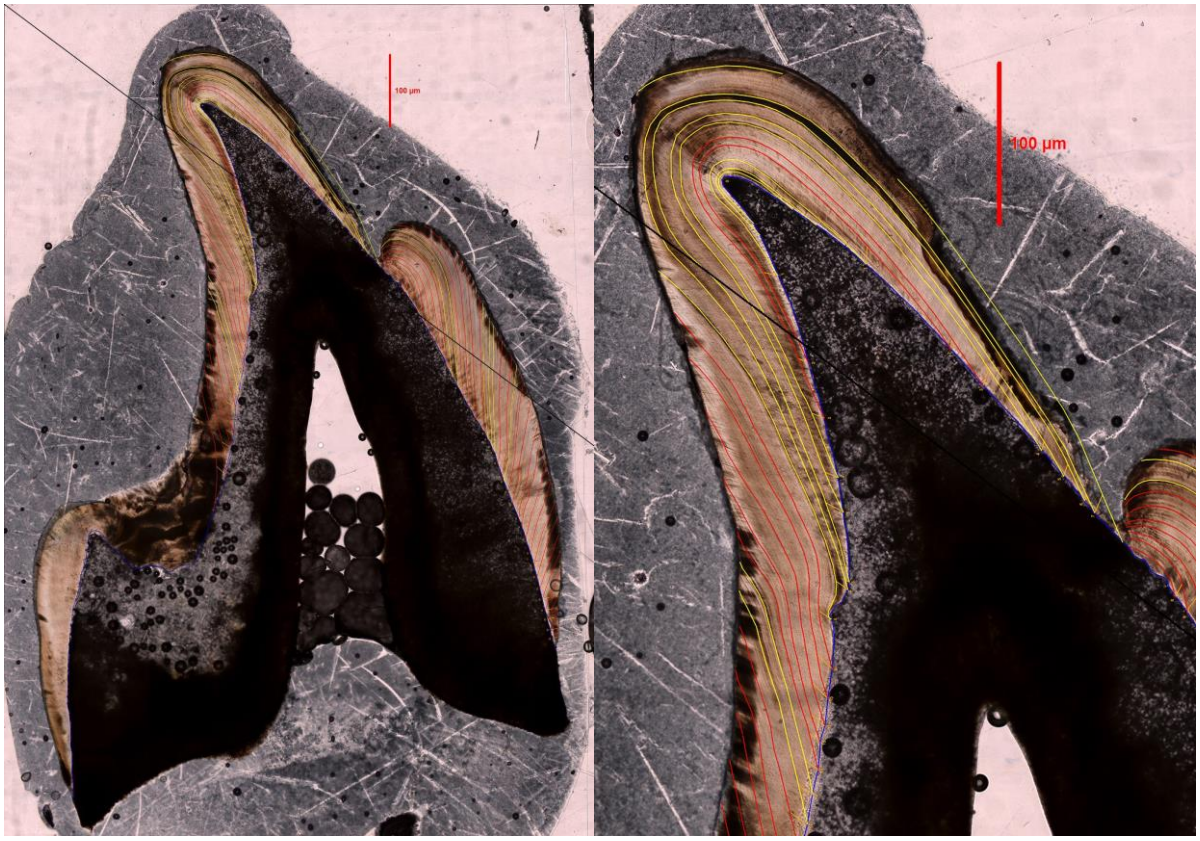

Fig. 16: Histological section of the upper right second incisor (URI2) of Individual 6. Left: view of the complete tooth. Right: view of the occlusal end in which the hypoplastic event is visible.

The average crown initiation time reported for the URI2 (383 days) by Reid and Dean (2006), was added to the timing of the hypoplastic event estimated by histological analysis (203 days; Table 4); the hypoplastic event occurred at age 585 days / 1.6 years when the crown was 2.7 mm long, or at 33% of crown completion. The total length of the EDJ on the buccal side equaled 8.2 mm over 1335 days. This corresponds to 44 months, or 3.7 years since crown initiation. The tooth crown was completely formed at 4.8 years of age when adding the crown initiation time of Read and Dean 2006 (383 days).

Landmarks	Cumulative Time Since Crown Initiation (Days)	Cumulative Time Since Crown Initiation (Months)	Time Before/After Hypoplastic Gap (Months)	Estimated Time Since Birth Based on Beginning of Crown Formation Time - 9 Months (Months)
AL 1	76.68	2.5	-9.2	11.5
AL 2	146.9	4.8	-6.9	13.8
AL 3	156.2	5.1	-6.6	14.1
AL 4	187.2	6.2	-5.5	15.2
AL 5	208.2	6.9	-4.8	15.9
AL 6	244.3	8.0	-3.7	17.0
AL 7	305.3	10.0	-1.7	19.0
AL 8	323.2	10.6	-1.1	19.6
AL 9	333.3	10.9	-0.7	20.9
AL 10 (Hypoplasia)	355.7	11.7	0.0	21.7
AL 11	481.4	15.8	2.9	23.6
AL 12	495.4	16.3	3.3	25.3
AL 13	591.7	18.5	6.5	27.5
AL 14	612.3	20.1	7.2	29.1
AL 15	767.9	25.2	12.3	34.2
AL 16	1172.7	38.5	23.6	47.5

Table 3: Timing of the ALs for the URC based on time since crown initiation (days and months), hypoplastic event, and birth. Estimated since birth based on Reid and Dean (2006). Cumulative time since the hypoplastic gap includes 37 days added after the hypoplastic gap, which is the estimated period since the initial hypoplastic event and when the enamel deposits resumed. Cumulative time since birth includes 75 days added after the hypoplastic gap, which is the estimated chronological gap.

Landmarks	Cumulative Time Since Crown Initiation (Days)	Cumulative Time Since Crown Initiation (Months)	Time Before/After Main Hypoplastic Event (Months)	Estimated Time Since Birth Based on Beginning of Crown Formation Time - 12.6 Months (Months)
AL 1 - 3	32.6	1.1	-6.7	13.7
AL 4	116.3	3.8	-3.9	16.4
AL 5	147.0	4.8	-2.9	17.4
AL 6	190.0	6.2	-1.4	18.8
AL 7 (Hypoplasia)	202.5	6.7	0.0	19.3
AL 8	234.1	7.7	1,0	20.3
AL 9	460.6	15.1	8.5	27.7
AL 10	497.1	16.3	9.7	28.9
AL 11	664.6	21.8	15.2	34.4
AL 12	688.4	22.6	16.0	35.2
AL 13	706.7	23.2	16.6	35.8
AL 14	791.0	26.0	19.3	38.6

Table 4: Timing of the ALs for the URI2 based on time since crown initiation (days and months), hypoplastic event, and birth. Estimated since birth based on Reid and Dean (2006).

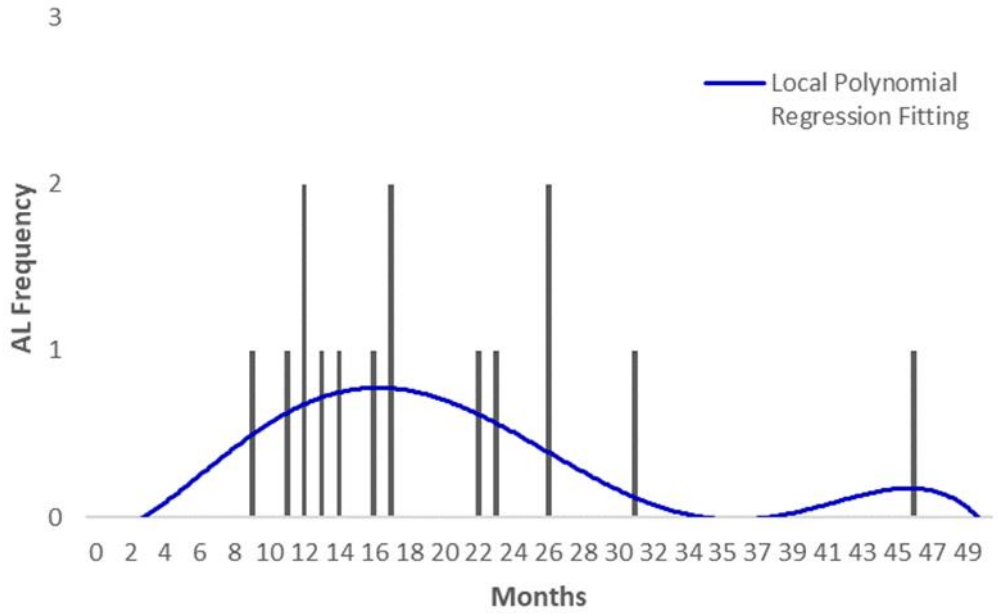

Fig. 18: Frequency of ALs per month in the URC of I1 from the beginning to end of crown formation using local polynomial regression fitting.

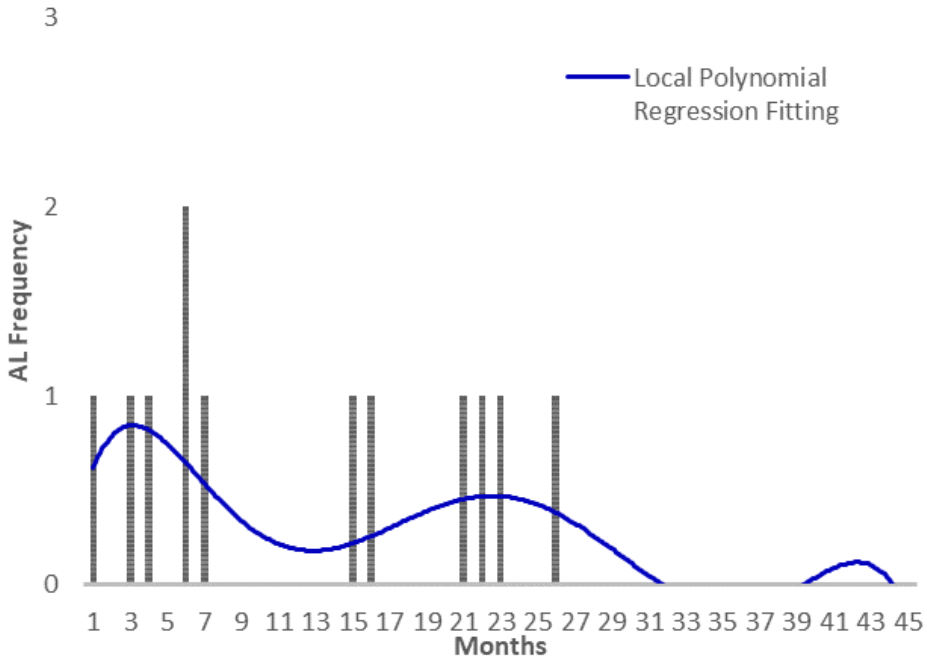

Fig. 19: Frequency of ALs per month in the URI2 in I6 from the beginning to end of crown formation using local polynomial regression fitting.

6. Discussion

6.1 Osteoarchaeological Analysis

The determined age at death for Individual 1 depended on the method that was used and varied between 16 and 20 years of age when using ossification and teeth eruption and 10 to 12 years of age when using bone length (Webb and Suchey, 1985; Garn et al., 1967; Cardoso, 2008; Coqueugniot and Weaver, 2007; AlQahtani, 2010; Moorrees, 1963; Brothwell, 1981; Black and Scheuer, 1996; Maresh, 1970). However, some of these estimates are more probable than others. A significant number of physiological stresses occurred within the first three years of life, as seen in Figure 15. The impact of these physiological stresses on teeth eruption and growth is generally less severe than its impact on limb bone growth, which may result in overall decreased growth or asymmetry (Kujanová, 2008; Macintosh, 2018). The age at death estimation is best reflected through teeth eruption, while the use of long bone length may reflect developmental age inaccurately. Therefore, it is more likely that this individual is around 18 years of age based on third molar eruption and enamel wear as opposed to around 12 years of age as suggested by long bone length. The ossification of the bones also supports this age estimation.

In the case of the infection that is present on the tibia and fibula in the same individual, the exact cause cannot be determined. The appearance suggests it may be a type of non-specific periostitis or potentially osteomyelitis given the location, which is commonly found on long bone extremities (Ortner, 2003). There is evidence of both a 1. healed infection and 2. a more recent infection - it is possible that the healed infection could have caused accentuated lines or even the hypoplasia itself in the canine before healing, although it is not known when this infection occurred during the individual's lifetime. Indeed, childhood viral infection has been seen as a cause of enamel hypoplasia (Nozaka, 1990).

In the case of Individual 6, one of the defining features of the teeth are the mamelons present on the central incisors. While this is a particularly common trait in children and especially in incisors, it is not possible to determine whether this feature is due to normal developmental variation or a feature of an enamel pathology (Chegini-Farahini, 2000; Kausar, 2020). However, as the molars also have abnormalities and they feature particularly high, pointed cusps, it could potentially be a feature of a dental condition affecting enamel growth and development, such as hypomineralization (Padavala, 2018). While the incisors appear more affected than the rest of the teeth (as is also the case with the canine of I1), it is recorded in literature that anterior teeth are particularly sensitive to physiological stress and are more likely to reflect such stress events through accentuated lines and hypoplasia (Dabrowski, 2021). It is therefore possible that the high cusps represent a high physiological stress event much like the hypoplasia in the upper lateral incisors.

6.2 Histology

Individual 1

The hypoplastic event of the URC occurred at 630 days / 1.7 years after birth. This time corresponds to 47% of EDJ length completion. We estimated the gap caused by hypoplasia in our Crown Formation Time (CFT) estimation to be between 75 and 93 days, meaning the total CFT of the URC is 4.9 years. This estimate is also supported by using the length of the EDJ and the EER between the same two points, which suggests 90 days passed. The period during which enamel secretion was interrupted was estimated to be around 37 days. It should be considered, however, that the enamel extension rate is far faster at the cuspal aspect of a tooth compared to the lateral aspect. As the equations used to estimate the chronological gap are based on the total crown formation time and not just the lateral formation times, this could mean that the estimations are slightly underestimated (Guatelli-Steinberg, 2012).

The initial timing of the hypoplastic event varies by two months between the lingual and buccal sides, occurring at 13.6 months and 11.6 months since the beginning of tooth formation, respectively. This may be because a standard DSR was used on both aspects. It is known that the lateral lingual aspect of a tooth has an on-average slower enamel extension rate than the buccal side, and so the use of a DSR where both aspects have the same rate may cause an apparent later timing of the hypoplastic event. However, the hypoplastic timing concerning its decile only differs by 1% (on the buccal side, it is at 47% of EDJ length completion, while on the lingual, it is at 46% EDJ length completion), and the hypoplastic gap on both sides between 2 and 3% of the total EDJ length. In fact, the calculated period of the hypoplastic gap differed by only 4 days (37 days for the buccal aspect and 41 days for the lingual) and only 5 days for the chronological gap (75 days for the buccal aspect and 80 days for the lingual). Both aspects of the crown also took the same amount of time to form (4.9 years). These two factors overall suggest the apparent difference in hypoplastic timing is due to variation in enamel secretion rates rather than a genuine variation in hypoplastic timing.

According to the chronology calculated using the Retzius lines and this estimated chronological gap, both the lingual and buccal sides suggest the crown was completed at age ~5.6 years. While this is longer than the average crown formation time for UCs of medieval samples as stated by Reid and Dean (2006) (4.5 years), this is entirely within the realm of probability according to AlQahtani (2010). While AlQahtani (2010), much like Reid and Dean (2006), does report UCs to be at the root initiation stage (RI) at 4.5 years, he also states that the minimum stage of development for the canine crown at 5 ½ years is Cr ¾, and it may even take up to 6 ½ years for the crown to be completed (AlQahtani, 2010).

Individual 6

The hypoplastic event of the URI2 occurred at 585 days / 1.6 years after birth. This time corresponds to 34non% of EDJ length completion.

According to the chronology calculated using the Retzius lines, the crown was completed at age 56 months / 4.7 years. While this is longer than the average crown formation time for URI2s as stated by Reid and Dean (2006) (4.1 years), this is entirely within the realm of possibility according to AlQahtani 2010. While AlQahtani (2010) does state that the root initiation stage (RI) can occur as early as 3.5 years (and thus crown completion before then), the minimum stage of development for the incisor crown at 4 ½ years is Cr ¾, and it may even take up to 6 ½ years for the crown to be completed (AlQahtani, 2010).

While this is longer than the average crown formation time for URI2s as stated by Reid and Dean (2006) (4.5 years), this is entirely within the realm of probability according to AlQahtani (2010). While AlQahtani (2010), much like Reid and Dean (2006), does report UCs to be at the root initiation stage (RI) at 4.5 years

Corresponding to Both Individuals

The results of the analysis correspond to other findings in histologically related studies of past populations, where accentuated lines are most frequent in the first several years of life, often due to conditions related to the process of weaning and introduction of new foods into the diet (Goodman and Rose, 1990; Kurek, 2022; Teivens, 1996). In the middle ages, weaning typically began around one year after birth and could take up to three years to complete (Dittman, 2000). At this time, the immune system is only about half the level seen among adults (Nava, 2018). This, combined with the decline of antibodies from the mother from breastfeeding, could introduce antigens and new pathogens to the developing child (Cummins and Thompson, 1997; Katzenburg et al, 1996; Mahoney, 2015). In both teeth, the hypoplastic events occurred at 1.7 years. The first accentuated line occurred for both individuals at around 1 year of age (11.5 months and 13.7 months for the URC and URI, respectively), which would be during the expected timing of the weaning process. For both individuals, nearly all accentuated lines occurred roughly within the first three years (for I1, nearly all accentuated lines occur in bulk before 2.9 years, excluding a single AL that occurred at 4 years. For I6, the last accentuated line occurs at 3.2 years). The number of accentuated lines, however, is higher than average for what has been recorded in literature for individuals with weaning periods of decent nutritional quality (Nava et al, 2018). If the increase in nutritional needs for the developing child had not been met, the physiological stresses seen through the accentuated lines and hypoplasia may indirectly be a result of the transition from weaning to solid foods. Malnutrition from non-nutritional solid food or an inadequate source of breast milk could potentially cause such hypoplasia, as general malnutrition and severe dietary deficiencies have been known to cause such defects (Folayan, 2020; Dabrowski, 2021). An inadequate source of breast milk,

which may result in severe malnutrition, diarrhea, and possibly lead to death, increases the severity of status until weaning is completed (Hühne-Osterloh and Grupe, 1989). Children in the second half of the first year of weaning are also the most susceptible to malnutrition (Dittmann and Grupe, 2000). Both of these factors may lend a possible explanation for the high frequency of accentuated lines in a single period of early childhood. However, without chemical analysis data on the teeth, it is not possible to come to this conclusion with complete certainty. Such malnutrition also further decreases the immune response, increasing the susceptibility to falling ill (Dittmann and Grupe, 2000).

Hypoplasia has also been found in those who were exposed to a severe health episode but survived (Boldsen, 2007). It is known that childhood illnesses can cause defects in permanent dentition, including hypoplasia, as a result of severe physiological stress (Reid and Dean, 2000; Dabrowski, 2021). At the time of the 1630s plague, there was a simultaneous outbreak of smallpox, a disease known to particularly affect children (Robb et al, 2021). This makes it possible that they may have been affected by smallpox depending on the length of the epidemic in the area, which could have made it possible that the individuals were affected when they were younger if the epidemic had already arrived during infancy. This is particularly true in the case of Individual 6 as it is younger and may have been exposed to this disease during the same wave of illness in early infancy. Diseases such as tuberculosis and leprosy, among other diseases of viral and bacterial origin are also associated with hypoplasia (King et al, 2002). Such diseases were common since the Middle Ages, and children were generally more vulnerable (Robb et al, 2021). It is therefore possible that any number of common diseases impacted these individuals during infancy, resulting in severe physiological stress and ultimately enamel hypoplasia. Such a disease may also explain the reduced skeletal development in Individual 1. If the stress was particularly strong, hypoplastic defects may appear on the surface of tooth crowns as well as in the roots, as a result of illness during childhood (Reid and Dean, 2000). This may explain not only the hypoplasia, but it could suggest the cause of the rather rapid development of dentine protuberances, which occur at the exact moment of enamel resumption after the hypoplastic event. Hypoplastic events have also been associated with higher mortality, making it possible that, if exposed to illness later in life, these two individuals may have been more susceptible to developing a severe and ultimately fatal disease (Boldsen, 2007). While it is impossible to say for certain if these individuals died due to the plague, the severity of their condition that resulted in death may in part be due to the stresses they accumulated during infancy. Further studies on other remains found on Lazzaretto Vecchio dated to the same time period, especially those that feature hypoplasia and/or a high number of ALs during infancy, may provide insight into this possibility.

7. Conclusion

The use of accentuated lines in dental histology allows us not only to identify periods of physiological stress but to reconstruct a chronological timeline of stress events in the early years of an individual's life. In the two individuals studied most of the ALs occurred during early childhood. Stress event prevalence occurred from approximately one to three years after birth, peaking between 1 ½ to 2 years for both individuals, with few stress instances occurring after 3 years. The number of ALs was also higher than what would be expected as "normal", or that of a relatively healthy individual with an adequate nutritional diet. If there were fewer accentuated lines, it could be proposed that the ALs may not indicate poor health, but rather the various non-fatal stresses that occurred during infancy (Nava et al, 2018). Non-fatal stresses during childhood are generally associated with the occurrence of various infectious diseases and dietary changes related to weaning (Nava et al, 2018). However, given the higher number of ALs and their increasing frequency around the hypoplastic events, plus the hypoplasia itself it is more likely that a more severe condition impacted these individuals. As both the ALs and the hypoplastic event occurred during the typical weaning time of the period, it is possible that they were indirectly a result of this process. Indeed, the weaning and immediate post-weaning periods have been reported to be a time of increased stress for children, including stressors such as a gradual loss of nutrients and immunity that would otherwise be supplied by human milk and an increase in contact with pathogens (Moggi-Cecchi, 1994). A nearly fatal illness may have caused the interruption of enamel secretion. While this alone is a high-stress event, it could also result in malnutrition if the child was unable to eat or digest properly, or if the food itself was of low nutritional value.

Given this, I propose that both the high frequency of ALs and the hypoplastic events arose during the particularly vulnerable weaning period and were likely the result of either a severe bout of illness, severe malnutrition, or an interactive combination of these factors. These stresses during infancy may have also resulted in higher susceptibility to fatal bouts of illness or disease, especially in the case of the plague.

Acknowledgments

Special thanks to Carla Figus and Antonino Vazzana for their mentorship in general osteoarchaeology and to Owen Higgins for his mentorship in dental enamel histology and continuous guidance and assistance throughout the research and writing process. Additional thanks to Alex Philiotis for image formatting.

References

Adler, C., Dobney, K., Weyrich, L. et al. Sequencing ancient calcified dental plaque shows changes in oral microbiota with dietary shifts of the Neolithic and Industrial revolutions. Nat Genet 45, 450–455 (2013). https://doi.org/10.1038/ng.2536

AlQahtani, Sakher & Hector, Mark & Liversidge, Helen. (2010). The London Atlas of Human Tooth Development and Eruption. American Journal of Physical Anthropology. 142. 481 - 490. 10.1002/ajpa.21258.

Anderson, T. Dental treatment in Medieval England. Br Dent J 197, 419–425 (2004). https://doi.org/10.1038/sj.bdj.4811723

Aris, Christopher. "Enamel Growth Rate Variation of Inner, Mid, and Outer Enamel Regions between Select Permanent Tooth Types across Five Temporally Distinct British Samples." Archives of Oral Biology, vol. 137, 2022, p. 105394., https://doi.org/10.1016/j.archoralbio.2022.105394.

Bifulco, M., Amato, M., Gangemi, G. et al. Dental care and dentistry practice in the Medieval Medical School of Salerno. Br Dent J 221, 87–89 (2016). https://doi.org/10.1038/sj.bdj.2016.528

Boldsen, Jesper L. "Early Childhood Stress and Adult Age Mortality—a Study of Dental Enamel Hypoplasia in the Medieval Danish Village of Tirup." American Journal of Physical Anthropology, vol. 132, no. 1, 2006, pp. 59–66., https://doi.org/10.1002/ajpa.20467.

Bramanti, B., Zedda, N., Rinaldo, N. et al. A critical review of anthropological studies on skeletons from European plague pits of different epochs. Sci Rep 8, 17655 (2018). https://doi.org/10.1038/s41598-018-36201-w

Brothwell, Don R. Digging up Bones: The Excavation, Treatment and Study of Human Skeletal Remains. British Museum (Natural History) and Oxford University Press, Oxford, 1981.

Chegini-Farahini, Sassan & Fuss, Janet & Townsend, Grant. (2000). Intra- and Inter-population Variability in Mamelon Expression on Incisor Teeth. Dental Anthropology. 14. 1-6. 10.26575/daj.v14i3.188.

Cobourne MT, Sharpe PT. Diseases of the tooth: the genetic and molecular basis of inherited anomalies affecting the dentition. Wiley Interdiscip Rev Dev Biol. 2013 Mar-Apr;2(2):183-212. doi: 10.1002/wdev.66. Epub 2012 May 25. PMID: 24009033.

Cornejo, OE. et al. Evolutionary and Population Genomics of the Cavity Causing Bacteria Streptococcus mutans, Molecular Biology and Evolution, Volume 30, Issue 4, April 2013, Pages 881–893, https://doi.org/10.1093/molbev/mss278

Cummins AG, Thompson FA. 1997. Review Article. Postnatal changes in mucosal immune response: a physiological perspective of breast feeding and weaning. Immun Cell Biol 75: 419–429.

Dąbrowski, Paweł, et al. “Estimation of Age at Onset of Linear Enamel Hypoplasia. New Calculation Tool, Description and Comparison of Current Methods.” Journal of Anatomy, vol. 239, no. 4, 2021, pp. 920–931., https://doi.org/10.1111/joa.13462.

Dean, KR., et al. “Human Ectoparasites and the Spread of Plague in Europe during the Second Pandemic.” Proceedings of the National Academy of Sciences, vol. 115, no. 6, 2018, pp. 1304–1309., https://doi.org/10.1073/pnas.1715640115.

de la Peña VA, Valea MC. Treatment of enamel hypoplasia in a patient with Usher syndrome. J Am Dent Assoc. 2011 Aug;142(8):938-41. doi: 10.14219/jada.archive.2011.0300. PMID: 21804060.

Dittmann K, Grupe G. Biochemical and palaeopathological investigations on weaning and infant mortality in the early Middle Ages. Anthropol Anz. 2000 Dec;58(4):345-55. PMID: 11190928.

Djurić-Srejić M and Stefanović S. “Tooth diseases in the medieval population of Gracanica near Valjevo” Srpski Arhiv za Celokupno Lekarstvo. 1998 Nov-Dec;126(11-12):430-436. PMID: 9921015.

Ell, SR. “Three Days in October of 1630: Detailed Examination of Mortality during an Early Modern Plague Epidemic in Venice.” Clinical Infectious Diseases, vol. 11, no. 1, 1989, pp. 128–139., https://doi.org/10.1093/clinids/11.1.128.

Folayan, MO et al. “Malnutrition, enamel defects, and early childhood caries in preschool children in a sub-urban Nigeria population.” PloS one vol. 15,7 e0232998. 1 Jul. 2020, doi:10.1371/journal.pone.0232998

Goodman, AH., and Rose, JC. “Assessment of Systemic Physiological Perturbations from Dental Enamel Hypoplasias and Associated Histological Structures.” American Journal of Physical Anthropology, vol. 33, no. S11, 1990, pp. 59–110., https://doi.org/10.1002/ajpa.1330330506.

Guatelli-Steinberg, D et al. “Enamel Extension Rate Patterns in Modern Human Teeth: Two Approaches Designed to Establish an Integrated Comparative Context for Fossil Primates.” Journal of Human Evolution, vol. 63, no. 3, 2012, pp. 475–486., https://doi.org/10.1016/j.jhevol.2012.05.006.

Gupta, P et al. “Role of sugar and sugar substitutes in dental caries: a review.” ISRN dentistry vol. 2013 519421. 29 Dec. 2013, doi:10.1155/2013/519421

Katzenberg MA, Herring DA, Saunders SR. 1996. Weaning and infant mortality: evaluating the skeletal evidence. Yrbk Phys Anthropol 101:177–199.

King, T et al. “A detailed study of enamel hypoplasia in a post-medieval adolescent of known age and sex.” Archives of Oral Biology, 47, 29–39. 2002, https://doi.org/10.1016/S0003 - 9969(01)00091 - 7

Kujanová, M et al. “Limb bones asymmetry and stress in medieval and recent populations of Central Europe” Int. J. Osteoarchaeol., 18: 476-491, 2008.. https://doi.org/10.1002/oa.958

Kurek, M, et al. “Time of Occurrence and Width of Accentuated Lines in the Enamel of Primary Incisors from Mediaeval Skeletal Remains from North-Central Poland: A Further Contribution to the Explanation of Early Childhood Mortality in Past Populations.” Journal of Archaeological Science, vol. 144, 2022, p. 105637., https://doi.org/10.1016/j.jas.2022.105637.

Lahtinen, M, and Salmi, AK. “Mixed Livelihood Society in IIN Hamina – a Case Study of Medieval Diet in the Northern Ostrobothnia, Finland.” Environmental Archaeology, vol. 24, no. 1, 2018, pp. 1–14., https://doi.org/10.1080/14614103.2018.1444695.

MacCord, K, "Biological Clocks and the Formation of Human Tooth Enamel". Embryo Project Encyclopedia (2013-01-31). ISSN: 1940-5030 http://embryo.asu.edu/handle/10776/4213.

Macintosh AA, Pinhasi R, Stock JT. “Early Life Conditions and Physiological Stress following the Transition to Farming in Central/Southeast Europe: Skeletal Growth Impairment and 6000 Years of Gradual Recovery.” PLOS ONE 11(2): e0148468, 2016. https://doi.org/10.1371/journal.pone.0148468

Magne P, Gallucci GO, Belser UC. Anatomic crown width/length ratios of unworn and worn maxillary teeth in white subjects. J Prosthet Dent. 2003 May;89(5):453-61. doi: 10.1016/S0022-3913(03)00125-2. PMID: 12806322.

Mahoney, P. “Dental Fast Track: Prenatal Enamel Growth, Incisor Eruption, and Weaning in Human Infants.” American Journal of Physical Anthropology, vol. 156, 2015, pp. 407–421., https://doi.org/10.1002/ajpa.22666.

Moggi-Cecchi J, Pacciani E, Pinto-Cisternas J. Enamel hypoplasia and age at weaning in 19th-century Florence, Italy. Am J Phys Anthropol. 1994 Mar;93(3):299-306. doi: 10.1002/ajpa.1330930303. PMID: 8042693.

Monson, TA., et al. “Neutral Evolution of Human Enamel–Dentine Junction Morphology.” Proceedings of the National Academy of Sciences, vol. 117, no. 42, 2020, pp. 26183–26189., https://doi.org/10.1073/pnas.2008037117.

Nava, A, et al. “Longitudinal Analysis of the Microscopic Dental Enamel Defects of Children in the Imperial Roman Community of Portus Romae (Necropolis of Isola Sacra, 2nd to 4th Century CE, Italy).” Journal of Archaeological Science: Reports, vol. 23, 2019, pp. 406–415., https://doi.org/10.1016/j.jasrep.2018.11.007.

Nozaka K, Sato T, Mukaida T, Shimazu A, Hasegawa J, Amari E. “Clinical study of enamel hypoplasia and its causes. 2. Permanent teeth.” Shoni Shikagaku Zasshi. 1990;28(3):579-99. Japanese. PMID: 2133960.

O’Neil, Ynez Violé. Medical Specialties and Disease Prevention. (1993). In K. Kiple (Ed.), The Cambridge World History of Human Disease. Cambridge: Cambridge University Press.

Ortner, Donald J. Identification of Pathological Conditions in Human Skeletal Remains. 2nd ed., Elsevier Academic, 2005.

Padavala S, Sukumaran G. Molar Incisor Hypomineralization and Its Prevalence. Contemp Clin Dent. 2018 Sep;9(Suppl 2):S246-S250. doi: 10.4103/ccd.ccd_161_18. PMID: 30294152; PMCID: PMC6169288.

Reid, D.J., and M.C. Dean. “Brief Communication: The Timing of Linear Hypoplasias on Human Anterior Teeth.” American Journal of Physical Anthropology, vol. 113, no. 1, 2000, pp. 135–139., https://doi.org/10.1002/1096-8644(200009)113:1<135::aid-ajpa13>3.0.co;2-a.

Reid, D.J., and M.C. Dean. “Variation in Modern Human Enamel Formation Times.” Journal of Human Evolution, vol. 50, no. 3, 2006, pp. 329–346., https://doi.org/10.1016/j.jhevol.2005.09.003.

Rev Infect Dis. 1989 Jan-Feb;11(1):128-41. doi: 10.1093/clinids/11.1.128. PMID: 2644686.

Robb, John & Cessford, Craig & Dittmar, Jenna & Inskip, Sarah & Mitchell, Piers. (2021). The greatest health problem of the Middle Ages? Estimating the burden of disease in medieval England. International Journal of Paleopathology. 34. 101-112. 10.1016/j.ijpp.2021.06.011.

Šlaus, M. (2000), Biocultural analysis of sex differences in mortality profiles and stress levels in the late medieval population from Nova Rača, Croatia. Am. J. Phys. Anthropol., 111: 193-209. https://doi.org/10.1002/(SICI)1096-8644(200002)111:2<193::AID-AJPA6>3.0.CO;2-0

Srejić, Marija Djurić. “Dental Paleopathology in a Serbian Medieval Population.” Anthropologischer Anzeiger, vol. 59, no. 2, 2001, pp. 113–22, http://www.jstor.org/stable/29541007.

Sun Zhe, Xu Lei, Schmid Boris V., Dean Katharine R., Zhang Zhibin, Xie Yan, Fang Xiye, Wang Shuchun, Liu Qiyong, Lyu Baolei, Wan Xinru, Xu Jianguo, Stenseth Nils Chr. and Xu Bing 2019Human plague system associated with rodent diversity and other environmental factorsR. Soc. open sci.6190216190216, http://doi.org/10.1098/rsos.190216

Tayles, N., et al. Agriculture and Dental Caries? The Case of Rice in Prehistoric Southeast Asia. World Archaeology, vol. 32, no. 1, Taylor & Francis, Ltd., 2000, pp. 68–83, http://www.jstor.org/stable/125047.

Teivens, A., et al. Enamel incremental lines as recorders for disease in infancy and their relation to the diagnosis of SIDS, Forensic Science International, Volume 81, Issues 2–3, 1996, Pages 175-183, ISSN 0379-0738, https://doi.org/10.1016/S0379-0738(96)01982-2.

Touger-Decker, R.; van Loveren, C; Sugars and dental caries, The American Journal of Clinical Nutrition, Volume 78, Issue 4, October 2003, Pages 881S–892S, https://doi.org/10.1093/ajcn/78.4.881S.

Towle, I; Davenport, C; Irish, J.D; De Groote; I. "Dietary and behavioral inferences from dental pathology and non-masticatory wear on dentitions from a British medieval town". bioRxiv 222091; doi: https://doi.org/10.1101/222091

Trombley, TM, Agarwal, SC, Beauchesne, PD, et al. Making sense of medieval mouths: Investigating sex differences of dental pathological lesions in a late medieval Italian community. Am J Phys Anthropol. 2019; 169: 253– 269. https://doi.org/10.1002/ajpa.23821

Valsecchi, M.C. (2007). "Mass Plague Graves Found on Venice "Quarantine" Island". National Geographic News. National Geographic Society. Retrieved October 22, 2010.

Van Hee, R. Wijzigingen in voedingsgewoonten en ziekteverschijnselen in de 16e en 17e eeuw [Changes in eating habits and disease symptoms in the 16th and 17th centuries]. Verh K Acad Geneeskd Belg. 1996;58(3):271-83. Dutch. PMID: 8848874.

Webb, Patricia A., and Judy Myers Suchey. "Epiphyseal Union of the Anterior Iliac Crest and Medial Clavicle in a Modern Multiracial Sample of American Males and Females." American Journal of Physical Anthropology, vol. 68, no. 4, 1985, pp. 457–466., https://doi.org/10.1002/ajpa.1330680402.

White, T. D., and Pieter A. Folkens. The Human Bone Manual. Elsevier Academic, 2005.

Woolgar, CM. The Senses in Late Medieval England. New Haven. Yale University Press. 2006. Pp. xi, 372. $40.00.

Wright JT, Carrion IA, Morris C. The Molecular Basis of Hereditary Enamel Defects in Humans. Journal of Dental Research. 2015;94(1):52-61. doi:10.1177/0022034514556708

Zabokova Bilbilova, Efka. (2020). Dietary Factors, Salivary Parameters, and Dental Caries. 10.5772/intechopen.92392.

Zanchetta, Letícia Maria Ramos et al. "Dental Anomalies in Individuals with Treacher Collins Syndrome – Tomographic Analysis." (2018).

Zechini, M; Killgrove, K; Melisch, C.M; Powers, N; Jungklaus, B; "Diet and Disease in Medieval Berlin: Dental Pathology Data from the Medieval Cemetery of Petriplatz." 2018.